

EXPECTED GAMMA SPECTRA AT ELI-NP-GBS

I. Drebot*, A. Bacci, C. Curatolo, A. Rossi, L. Serafini, INFN Milano
 V. Petrillo, Università degli Studi di Milano & INFN, Milano
 C. Vaccarezza, A. Variola, INFN/LNF, Frascati Roma
 A. Giribono, University of Rome “La Sapienza”, Rome

Abstract

The ELI-NP-GBS is an advanced source of up to 20 MeV Gamma Rays based on Compton back-scattering. We present the investigation of the production of the ELI-NP gamma photon beam generated by Compton back-scattering between the electron bunch accelerated in the linac and the laser pulse. At the interaction point (IP), the Compton backscattering properties, as spectral flux, brilliance and polarization are evaluated by the Klein-Nishina cross section. The gamma beam produced has energy ranging from 0.2 to 19.5 MeV and bandwidth of 0.5%. In order to define the optimal layout and evaluate the performances of the collimation and detection systems, a detailed Monte Carlo simulation activity has been carried out taking into account possible jitters and errors.

INTRODUCTION

The European Extreme Light Infrastructure (ELI) dedicated to Nuclear Physics/Photonics (ELI-NP) Gamma Beam System (ELI-NP-GBS) is one of the three pillars of ELI European Project [1], [2]. ELI-NP-GBS is presently under construction in Magurele (Romania).

The ELI-NP-GBS is an intense and monochromatic gamma source based on Compton back scattering between a high-power laser and an accelerated electron beam produced by linac [3]. The photon beams, in the 1-20 MeV energy range, are characterized by unprecedented performances in terms of mono-chromaticity, brilliance, spectral density, tunability and polarization.

The main specifications of the Compton Source of gamma ray photon beams are, in fact, mono-chromaticity less than 0.5%, peak brilliance larger than $10^{21} N_{ph}/(s \cdot 0.1\% \cdot \text{mm}^2 \cdot \text{mrad}^2)$, large tunability, fully controlled polarization, spectral density larger than $10^4 N_{ph}/(s \cdot \text{eV})$ and focused down to micron-scale spot sizes. It can open several novel horizons in the photon-photon and photon-particle collider scenarios.

Due to the up-shift of the energy of the backscattered photons up to the cut off energy $E_\gamma = 4\gamma^2 E_{laser}$ where gamma is the relativistic factor: $\gamma = E_e[\text{MeV}]/0.511$, E_e is electron beam energy in MeV, in the ELI NP GBS it will be possible to produce gamma rays up to ~ 20 MeV with maximum electron beam energy of 750 MeV.

The main parameters of the electron, laser and gamma beams are listed in table 1 and 2.

* illya.drebot@mi.infn.it

LASER SYSTEM

The lay-out of the laser recirculator for ELI-NP-GBS is presented in Fig. 1. It is made by two confocal parabolic mirrors and 32 plane mirror pairs to focus, deflect, collimate and recirculate the J-class green light Yb:Yag laser pulse for collision at IP (at the center of the device) with each of the 32 electron bunches accelerated to the IP by the multi-bunch RF Linac [4]. The parameters of laser pulse are presented in Table 1.

Table 1: Parameters of the Laser System

Pulse energy (J)	0.2; 0.4
Wave length [nm]	515
Pulse length [psec]	1.5
Focal spot size w_0 RMS [μm]	28
Laser parameter a_0	0.02; 0.04
Collision angle [deg]	8

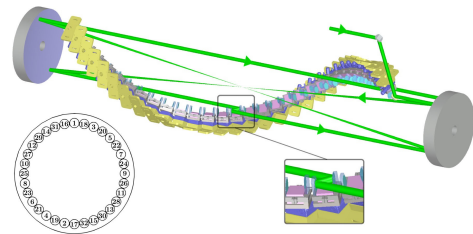


Figure 1: Lay-out of the laser recirculator for ELI-NP-GBS.

COLLIMATION SYSTEM

To assure a good monochromaticity to the gamma ray beam a system of collimators will be implemented and integrated in the system. It will cut most of the produced flux up to $\approx 98.5\%$. The result will be the production of a tunable gamma source, between 0.2 and 19.5 MeV photons, with a 0.5 % bandwidth. Number of scattering photons, bandwidth and Stokes parameters for the scattered photons as function of the acceptance angle for for 2 MeV photons beam are presented in the Fig. 2.

POLARIZATIONS

The polarization degree is connected to the momentum distribution of the photons, so the polarization shape appears only after propagation of the photons up to the far zone [5]. The results show that, while for a bandwidth (BW) $BW = 5 \cdot 10^{-3}$ the beam of scattered photons is polarized at 99.9%, for application requiring higher flux and larger BW,

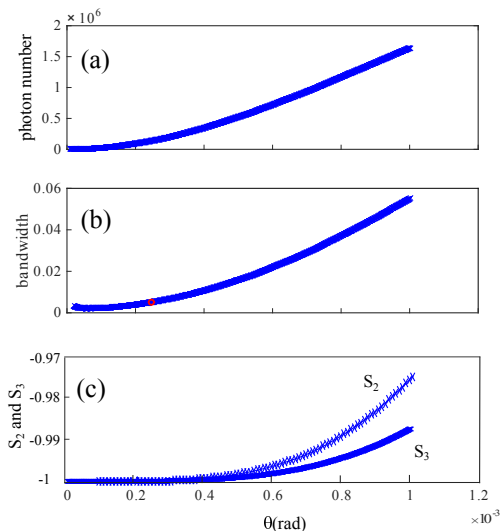


Figure 2: Number of scattering photons (a), bandwidth (b) and Stokes parameters (c) for the case of linear (S3) and circular (S2) polarizations as function of the acceptance angle. The red dot marks the bandwidth 0.5%.

the polarization deteriorates. In Fig. 3, a synthetic view of both intensity and polarization is shown for several ELI-NP working points.

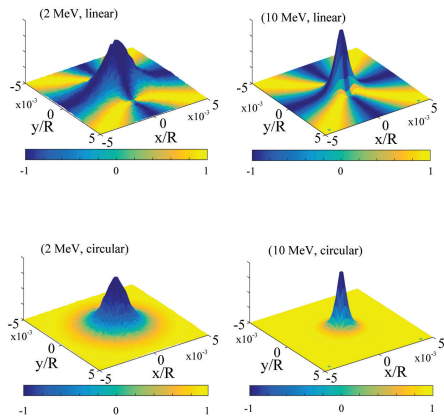


Figure 3: Intensity-polarization graphs for photons at 2 and 10 MeV, with linear and circular laser polarization.

ERRORS AND JITTERS EFFECTS ON RADIATION

In the framework of simulation of the spectrum of scattered photons the analysis was done of the influence of possible positions and orientation misalignment of the laser pulse at the interaction point of the ELI-NP project. In the Fig. 4 the degradation of the total number of emitted photons due to the longitudinal displacement of the laser beam at IP is presented. The asymmetry in the flux degradation is due to collision angle, that is in the x-plane 8 deg and in y-plane is 0 deg.

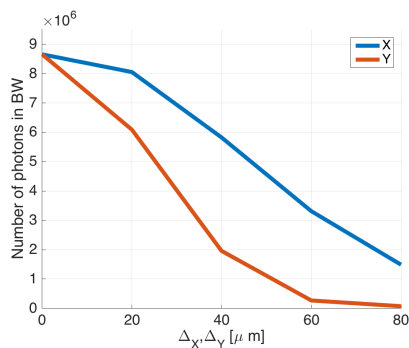


Figure 4: Number of emitted photons with BW 0.5% as a function of the transverse misalignments.

The longitudinal misalignment in the considered range have lower impact on the photon flux with respect to the transverse ones, see Fig. 5. The misalignment in the longitudinal plane has no effects on the BW and on polarization and it can be compensated by the synchronization.

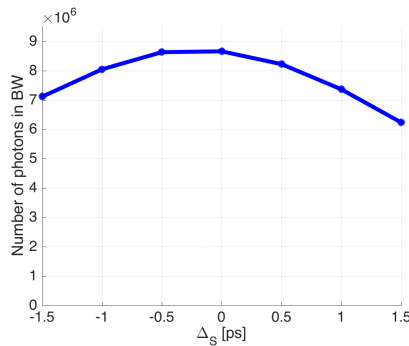


Figure 5: Number of emitted photons with BW 0.5% as a function of the longitudinal misalignments.

The collimation system is installed at 10 m from the IP. In the Fig. 6 the increasing of the BW of scattered photons due to the transverse misalignments of collimation system is presented. We can see that until 200 micrometers this changes are negligible.

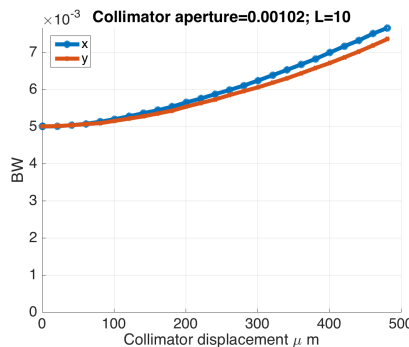


Figure 6: BW as a function of the transverse misalignments of collimation system.

Table 2: Main Working Points

	0.2 MeV	1 MeV	2 MeV	3.5 MeV	10 MeV	13 MeV	19.5 MeV
Electron beam Parameters							
Electrons mean energy [MeV]	74.9	165	234.2	311.7	529.8	604.8	750
Bunch charge [pC]	250						
Bunch length rms [μm]	275	271	273	278	271	272	278
Nominal normalized $\epsilon_{nx}, \epsilon_{ny}$ [mm.mrad]	0.51; 0.43	0.47; 0.43	0.43, 0.41	0.41; 0.4	0.43; 0.43	0.43, 0.43	0.4; 0.4
Nominal relative energy spread σ_e %	0.11	$9.4 \cdot 10^{-2}$	$8.1 \cdot 10^{-2}$	$8 \cdot 10^{-2}$	$4.4 \cdot 10^{-2}$	$4.3 \cdot 10^{-2}$	$4.8 \cdot 10^{-2}$
Focal spot size σ_x, σ_y μm	23.4; 23.4	20.6; 19.1	19.5, 19.5	19.2; 19.3	17.2; 16.4	17.1; 16.6	15.9; 15.9
γ -ray Photon Beam Parameters							
Peak, Mean of spectrum [MeV]	0.2; 0.2	0.998; 0.995	1.98; 1.98	3.51; 3.5	10; 10	13.1; 1.3	20; 20
Collimation angle θ_{max} [μrad]	717	328	229	175	92	74	64
Bandwidth [KeV]	1.03	5.07	10	17.7	51	66.2	100
Bandwidth	$5.08 \cdot 10^{-3}$	$5.09 \cdot 10^{-3}$	$5.07 \cdot 10^{-3}$	$5.06 \cdot 10^{-3}$	$5.08 \cdot 10^{-3}$	$5.07 \cdot 10^{-3}$	$5.04 \cdot 10^{-3}$
Nominal # photons per shot after collimation N_{ph}	$9.76 \cdot 10^4$	$1.46 \cdot 10^5$	$1.36 \cdot 10^5$	$1.36 \cdot 10^5$	$2.41 \cdot 10^5$	$2.08 \cdot 10^5$	$2.33 \cdot 10^5$
Nominal # photons/sec after collimation	$3.12 \cdot 10^8$	$4.68 \cdot 10^8$	$4.37 \cdot 10^8$	$4.38 \cdot 10^8$	$7.72 \cdot 10^8$	$6.66 \cdot 10^8$	$7.48 \cdot 10^8$
Nominal Spectral Density Nph/(sec*eV)	$1.19 \cdot 10^5$	$3.68 \cdot 10^4$	$1.73 \cdot 10^4$	$9.84 \cdot 10^3$	$6.03 \cdot 10^3$	$4.01 \cdot 10^3$	$2.96 \cdot 10^3$
Time-Average Peak Spectral Density at Peak Energy	$9.41 \cdot 10^4$	$3.75 \cdot 10^4$	$1.85 \cdot 10^4$	$1.05 \cdot 10^4$	$7.84 \cdot 10^3$	$6.07 \cdot 10^3$	$4.18 \cdot 10^3$
Source rms size $\sigma_{\gamma x}, \sigma_{\gamma y}$ [μm] at IP	20.6; 14.3	18.2; 10.6	16.8; 11.2	16.7; 11.2	16.2; 10.5	15; 1.01	15.5; 10.5
Source rms $\sigma_{\gamma X'}, \sigma_{\gamma Y'}$ divergence [μrad]	356; 355	162; 163	115; 113	86.9; 86.4	46.2; 45.6	37; 3.66	32; 31.8
Source rms divergence θ_{RMS} [μrad]	502	230	161	122	64.9	52.1	45.1
Spot Size at 10 m [mm]	3.56; 3.55	1.62; 1.63	1.15, 1.13	0.86; 0.86	0.46; 0.45	0.37; 0.36	0.32; 0.31
Rad. pulse length $\sigma_{\gamma z}$ [psec]	0.86	0.83	0.81	0.83	0.82	0.81	0.84
brilliance peak	$6.46 \cdot 10^{18}$	$7.08 \cdot 10^{19}$	$1.37 \cdot 10^{20}$	$2.32 \cdot 10^{20}$	$1.64 \cdot 10^{21}$	$2.49 \cdot 10^{21}$	$3.37 \cdot 10^{21}$
brilliance average	$4.49 \cdot 10^{10}$	$4.72 \cdot 10^{11}$	$9 \cdot 10^{11}$	$1.55 \cdot 10^{12}$	$1.08 \cdot 10^{13}$	$1.62 \cdot 10^{13}$	$2.29 \cdot 10^{13}$

CONCLUSION

The future availability of advanced X/ γ ray photon beams in the energy range 1-20 MeV range will open many opportunities of addressing strategic applications in Nuclear Photonics, performing experiments of fundamental physics in QED. Open problems and set-up for new sources of pion, muon and neutrino beams based on pion photo-production on highly relativistic proton beams (LHC-like) can be studied. The EuroGammaS collaboration is building the most advanced source in this field that will start operation in 2018.

REFERENCES

- [1] "ELI-Extreme Light Infrastructure", <http://www.eli-laser.eu/>, 2014.
- [2] "ELI-Nuclear Physics", <http://www.eli-np.ro/>, 2014.
- [3] O. Adriani *et al.*, "Technical Design Report EuroGammaS Proposal for the ELI-Gamma Beam System", arXiv:1407.3669, 2014.
- [4] K. Dupraz *et al.*, in *Phys. Rev. ST Accel. Beams*, vol. 17, p. 033501, 2014.
- [5] Petrillo V. *et al.*, in *Phys. Rev. ST Accel. Beams*, vol. 18, p. 110701, 2015.